

Discrete charge transfer in nanoparticle solid films

Shaowei Chen*

DOI: 10.1039/b707884f

A brief overview of the recent progress in single electron transfer (SET) in nanoparticle solid films is presented. In these studies, Langmuir-based techniques were employed to control the interparticle interactions, and the ensemble conductivity was evaluated by electrochemical measurements. Deliberate manipulation of the ensemble structure and temperature led to the optimization of the conductivity properties where SET was initiated across a nanoparticle solid film.

One of the unique properties of organically capped transition-metal nanoparticles^{1–6} is their molecular capacitance characters, which have been hailed as the fundamental basis for the development of single electron transistors.⁷ Conventionally, these are manifested as the Coulomb staircase phenomenon in scanning tunneling spectroscopic (STS) studies of isolated particles,^{8–10} as interpreted by the double-junction model. In electrochemical studies, analogous behavior has also been observed in electrolyte solutions with nanoparticles of selected size and narrow dispersity,³ which are represented by a series of well-defined and (almost) evenly spaced voltammetric peaks. From the peak potential spacing (ΔV) the nanoparticle molecular capacitance can be estimated ($C_{MPC} = e/\Delta V$,

with e being the electronic charge). More interestingly, for nanoparticle ensembles in aqueous solutions, these discrete charge-transfer processes can be rectified by hydrophobic electrolyte anions,¹¹ which is ascribed to the manipulation of the electrode double-layer capacitance by the ion-pair formation between nanoparticles and electrolyte ions. To render the systems more relevant to device applications, extension into solid-state electrochemistry is desired. However, studies of quantized charge transfer in nanoparticle solid assemblies have remained scarce so far. The progress is primarily impeded by the fact that in the solid state, the nanoparticle electronic conductivity is the combined consequence of a large number of structural parameters, and hence far more complicated than in STS measurements of a single particle and in electrochemical studies where the interparticle interactions are essentially minimal.

In nanoparticle solids, the ensemble conductivity is the interplay of at least

three effects:¹² (i) the disorder due to the dispersity of particle core size, shape and chemical environments, (ii) the (dipolar) exchange coupling between adjacent particles, and (iii) the Coulomb repulsion of electrons (of opposite spins) on a given particle. In these, the disorder within the particle ensembles will diminish the interparticle electronic coupling. Consequently, the electronic wavefunctions will be localized within individual nanoparticles because of the overwhelming Coulombic barrier to charge migration, leading to low conductivity of the particle solids. Thus, it can be envisioned that the interparticle charge transfer will encounter low energetic barriers for strongly coupled nanoparticle ensembles, leading to high conductance; whereas low conductance is anticipated for weakly coupled systems. So the questions arise, how does one effectively control the electronic coupling of nanoparticles so that their charge transfer properties can be readily manipulated? And more importantly, at what point can discrete charge transfer be observed?

In the studies of nanoparticle solid ensembles, the Langmuir-based techniques are commonly used to fabricate monolayers and multilayers at controlled interparticle distances,¹³ whereas (sub)-micrometer-thick solid films are typically prepared by dropcasting/spincoating a particle solution in a volatile organic solvent onto a flat electrode surface.^{14–19} In the latter, the ensemble conductance has been found to be primarily driven by the thermally activated percolation effect as well as core thermal motions.¹⁴

Department of Chemistry and Biochemistry,
University of California, 1156 High Street,
Santa Cruz, California 95064, USA.
E-mail: schen@chemistry.ucsc.edu



Shaowei Chen

Shaowei Chen finished his undergraduate studies in 1991 with a BS degree in Chemistry from the University of Science and Technology of China, and then went to Cornell University receiving his MS and PhD degrees in 1993 and 1996 respectively. Following a postdoctoral appointment in the University of North Carolina at Chapel Hill, he started his independent career in Southern Illinois University at Carbondale in 1998. In summer 2004, he joined the faculty of the University of California at Santa Cruz, and is currently an associate professor of chemistry.

Because of rampant structural inhomogeneity (disordering) within these particle thick films, the energetic barriers for interparticle charge transfer most likely vary widely from site to site. Consequently, typically only featureless linear (ohmic) I - V behavior is observed, especially at a relatively high voltage bias. Note that in these systems, the interparticle spacing is presumably fixed by the organic surfactant layers that protect the individual nanoparticle cores as a consequence of ligand intercalation; however, the reproducibility of the particle film structure may be compromised because of the crude nature of the preparation method. Thus, they do not appear to be feasible candidates to achieve solid-state single electron transfer.

As the structural intermediate between isolated particles and particle multilayers (thick films), particle monolayers exhibit very unique electronic conductivity properties. For instance, particle monolayers have been prepared at the air/water interface by the Langmuir method, and the interparticle separation can be accurately controlled by mechanical compression,²⁰ leading to a relatively large range of manipulation of the interparticle interactions, in sharp contrast to the dropcast thick films mentioned above. Consequently one can achieve an unprecedented degree of deliberate control of interparticle electronic coupling and hence the resulting ensemble I - V characteristics. One well-known example is the insulator-metal transition observed by Heath and coworkers^{4,21} and others²² in the studies of the electrical characteristics of a Langmuir monolayer of alkanethiolate-protected silver (AgSR) nanoparticles at the air/water interface, when the particle monolayer was mechanically compressed to a sufficiently small interparticle spacing.

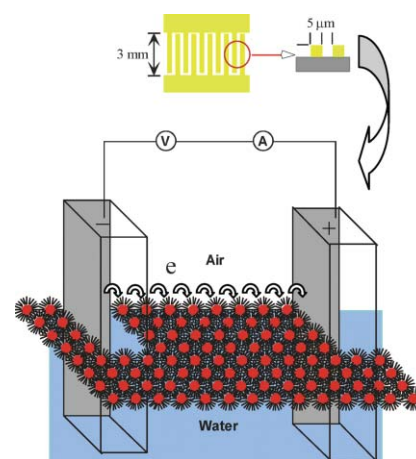
The electronic conductivity of gold nanoparticle *monolayers* either on the water surface or on solid substrates has also been reported.^{23–26} However, in these earlier studies, the conductivity profiles exhibited no characteristics of *quantized charging* of the particle molecular capacitance. It should be noted that the fundamental physics behind the discrete charging/discharging processes is attributable to the (sub)attofarad (aF) molecular capacitance (C_{MPC}) of these

nanoentities, which renders the energetic barrier ($e^2/2C_{\text{MPC}}$) for single electron transfer larger than the thermal kinetic energy ($k_{\text{B}}T$, k_{B} the Boltzmann constant). As C_{MPC} is determined by the particle structure,²⁷

$$C_{\text{MPC}} = 4\pi\epsilon\epsilon_0 \left(\frac{r}{d}\right) (r+d) \quad (1)$$

where ϵ is the (effective) dielectric constant of the particle protecting monolayer, ϵ_0 is the vacuum permittivity, r is the particle core radius and d is the thickness of the protecting monolayer, one can see that nanoparticle quantized charging can only be observed either at low temperature and/or with ultrasmall particle molecules. Our previous studies have shown that the nanoparticle core diameter must be <2.5 nm in order to observe quantized charging behavior in solution at ambient temperature.²⁷ Thus, we anticipate a similar size range for solid-state studies. In the above studies with Ag or Au particle monolayers,^{4,21–26} most of the particles were too big and/or too polydisperse, and consequently no quantized charging was observed in these particle films.

The recent rapid advancement in syntheses has resulted in the ready availability of (almost) monodisperse and ultrasmall (diameter <3 nm) gold particles, rendering it possible to fabricate a clearly defined ensemble structure for the studies of their solid-state electron-transfer properties. In fact, single electron transfer can now be achieved with monolayers of these particles at controlled interparticle arrangements. For instance, using the Langmuir technique,^{28,29} we have studied the electronic conductivity of a series of gold nanoparticles (core diameter 2 nm, with dispersity $<20\%$) with varied protecting ligands, and observed drastic differences in the I - V profiles with the variation of the structures of the particles and their ensembles. The experimental setup is shown in Scheme 1. Specifically, the I - V characteristics of the nanoparticle monolayers are examined *in situ* at varied surface structures by using an interdigitated array electrode (IDA, consisting of 25 pairs of gold fingers, $5\ \mu\text{m} \times 5\ \mu\text{m} \times 3\ \text{mm}$ with a $5\ \mu\text{m}$ gap, Scheme 1 top) vertically aligned at the air/water interface. It should be noted that *the subphase contains only Nanopure water ($>18\ \text{M}\Omega$)*



Scheme 1 Schematic of conductivity measurements of a nanoparticle monolayer at the air/water interface. Inset shows the schematic configuration of an IDA electrode. Reproduced with permission from the American Chemical Society (ref. 29).

without any added electrolyte. This is fundamentally different from the horizontal touch voltammetry (HTV) technique that was developed by Fujihira and Araki³⁰ and Majda *et al.*²⁵

Fig. 1A shows the I - V responses of a monolayer of n-butanethiolate-passivated gold (C4Au) nanoparticles at varied interparticle spacing at the air/water interface (interparticle edge-to-edge distance, L , was calculated from the Langmuir isotherm, by assuming a hexagonal close-packed structure). In comparison to the control experiment in the absence of the nanoparticle monolayer (“blank”), the currents measured are substantially greater, and increase with decreasing interparticle spacing. The linear (ohmic) characters of the observed conductance profiles suggest strong interparticle coupling (*vide infra*). The conductivity evaluated from the slope is of the order of $10^{-3}\ \text{S cm}^{-1}$ (Fig. 1B) which is about 8 orders of magnitude smaller than that for bulk gold ($4.43 \times 10^5\ \text{S cm}^{-1}$ at ambient temperature),³¹ indicative of semiconductor electrical characteristics of the nanoparticle monolayer films due to the nanoscale organic/inorganic composite structure. Nonetheless, the result is comparable to those of (micrometer) thick films of gold nanoparticles of similar core sizes and protecting alkanethiolate layers.^{14–19} In addition, the conductivity decreases exponentially with increasing interparticle distance (Fig. 1B) suggesting a

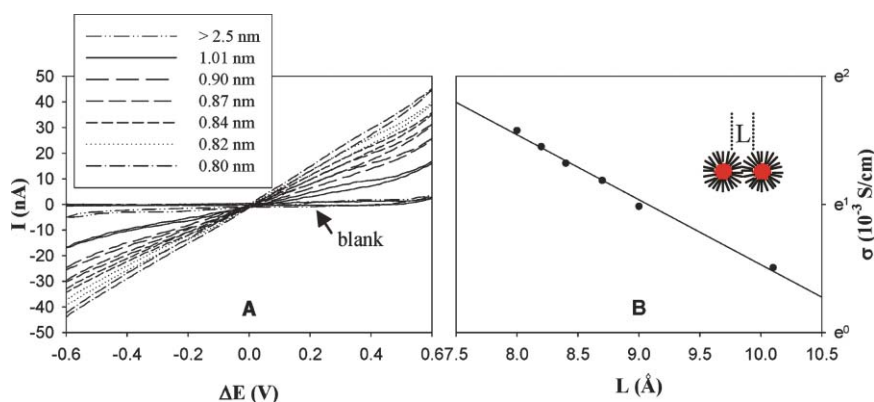


Fig. 1 (A) I - V curves of a C4Au nanoparticle monolayer at varied edge-to-edge interparticle distances (L) which are shown as figure legends. The label “blank” refers to the control experiment in the absence of nanoparticle monolayers. Potential scan rate 10 mV s^{-1} . (B) Variation of electronic conductivity with the interparticle spacings. Symbols are experimental data and line is the linear regression. Reproduced with permission from Elsevier (ref. 28).

hopping mechanism of the interparticle charge transfer, with a decay coefficient (β) of about 0.5 \AA^{-1} . The β value is somewhat smaller than those typically found with nanoparticle dropcast thick films ($\beta = 0.8\text{--}1.2 \text{ \AA}^{-1}$).^{14–19} This may be, partly, ascribed to the long-range ordering within the particle monolayers and hence enhanced interparticle electronic coupling because of the low dispersity of core size.

Note that the electronic conductivity of a nanoparticle molecule is governed by at least two factors, the core and the protecting monolayer, which are reflected by the effects of Coulomb blockade and electron tunneling, respectively.³² In the present study, the bandgap of the particle molecules is anticipated to be insignificant because the particle core size is not sufficiently small;³ thus, the collective conductance of the nanoparticle assemblies is mainly determined by electron hopping between neighboring particles, where the β value reflects the combined effects of the organic insulating layer (tunneling barrier) and the electronic interactions between neighboring particle cores.

Similar linear I - V responses were also observed with the Langmuir monolayers of *n*-pentanethiolate-protected gold (C5Au) particles.²⁸ However, for particles protected by longer alkanethiolates, the I - V profiles exhibited a substantial deviation from the linear characteristics. Fig. 2 shows the I - V curve of a Langmuir monolayer of *n*-hexanethiolate-protected gold (C6Au) particles at the air/water interface with L equal to one hexyl spacer (0.77 nm, *i.e.*,

the particles are fully intercalated). First, it can be seen that the I - V profile is highly nonlinear; and within the potential range of -1.2 to $+0.6$ V, the voltammetric current is very small, only of the order of a few tens of nA, whereas at more positive potentials, the current starts to rise very rapidly (the asymmetric appearance of the I - V profile most probably arises from disordered domains within the particle monolayers on the water surface). Such behavior is analogous to Coulomb blockade but very different from that observed above with particles protected by monolayers of shorter alkanethiolates (*e.g.*, C4Au and C5Au, Fig. 1) that exhibit mostly linear I - V responses.²⁸ More interestingly, there exist several features within the bias range of -0.5 to $+1.0$ V, with at least four very well-defined current peaks at -0.30 , $+0.17$, $+0.48$, and $+0.93$ V (indicated by asterisks). We ascribe these peaks to the *sequential single electron transfer across the nanoparticle monolayer* (Scheme 1). From the peak spacing ($\Delta V \approx 0.40$ V), the effective particle-to-particle capacitance (C_{PP}),[†] 0.40 aF, can

[†] Because of the close proximity and electronic interactions between particles, the capacitance evaluated here most probably reflects the capacitive coupling between neighboring particles (C_{PP}); whereas C_{MPC} (eqn (1)) denotes the molecular capacitance of individual particles with negligible interparticle interactions. This is a key fundamental difference between solid state and solution electrochemistry of nanoparticle quantized charge transfer. There is no analytical expression for the coupled capacitance between two spherical capacitors.

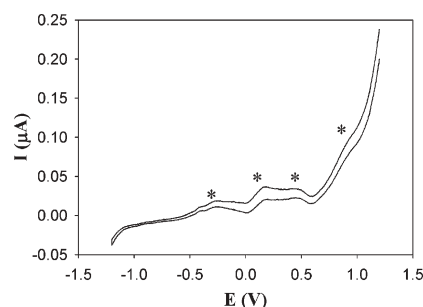


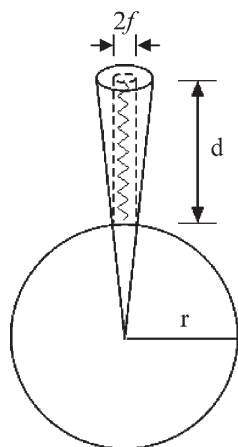
Fig. 2 I - V profile of a C6Au nanoparticle monolayer at the air/water interface with the interparticle (edge to edge) separation equal to one hexyl spacer (*i.e.*, the particles are fully intercalated). Experimental conditions are the same as in Fig. 1.

be estimated at this specific monolayer structure. For comparison, for *n*-decane-thiolate-protected gold (C10Au) particles, when the particles were fully intercalated, $\Delta V = 0.42$ V, and $C_{PP} = 0.38$ aF.²⁹ Overall, ΔV decreases and C_{PP} increases with shrinking interparticle separation (L), due to the enhanced interparticle electronic interactions.

The above results^{28,29} can be rationalized by the particle monolayer structure, where the phase behavior of the particle Langmuir monolayers has been found to be mainly defined by the particle core size and the chemical structures of the protecting ligands.³³ Heath *et al.* have shown that the variation of the phase behavior can be discussed in terms of the extra (conical) volume (V_e) available to the alkyl capping group as it extends from a nearly spherical metal core (Scheme 2),³³ with

$$V_e = \frac{\pi}{3} \left(\frac{f}{r} \right)^2 \left[(r+d)^3 - r^3 \right] - \pi d f^2 \quad (2)$$

where f is the footprint radius of the ligands on the core surface (and πf^2 represents the footprint area which for alkanethiolates on gold³⁴ is 0.214 nm^2), and others have been defined in eqn (1). Three distinct phases of metal nanoparticle monolayers have been identified.³³ For $V_e > 0.35 \text{ nm}^3$, the Langmuir monolayers are dominated by extended, low-dimensional structures that, at high surface pressures, compress into a two-dimensional foam-like phase as a result of ligand intercalation. For $0.15 \text{ nm}^3 < V_e < 0.35 \text{ nm}^3$, the dispersion attraction of the metal cores induces condensation



Scheme 2 Schematic representation of the extra (conical) volume for ligands adsorbed on a nanoparticle surface. Reproduced with permission from the American Chemical Society (ref. 33).

of the particles to form close-packed structures (crystalline phases). At even smaller V_e ($<0.15 \text{ nm}^3$), the particles irreversibly aggregate into highly packed structures. Such phase evolution has been elucidated by TEM measurements of nanoparticle Langmuir–Blodgett (LB) monolayers,³³ suggesting structural integrity of the particle films during the deposition process.

Table 1 lists the corresponding extra volumes for gold nanoparticles (core diameter 2 nm) protected with varied alkanethiolate monolayers that were used in the above studies.^{28,29} Three points warrant attention here. First, the linear (ohmic) I – V characteristics observed above (Fig. 1) with the C4Au and C5Au particles may be ascribed to the highly packed ensemble structures as manifested by their very small V_e s. Second, the transition to nonlinear I – V behavior coincides with the C6Au particles where the V_e value is slightly greater than 0.15 nm^3 and long-range ordered structures are obtainable with controllable interparticle separation. Third, for particles with very long alkanethiolate chains (e.g., C10Au, $V_e > 0.35 \text{ nm}^3$), the foam-like structures of the particle monolayer suggest that the actual interparticle distance may be smaller than that calculated from the Langmuir isotherm (which is essentially a macroscopic average). Thus, the particle-to-particle capacitance (C_{PP}) estimated above²⁹ for the C10Au ensemble may actually correspond to an interparticle distance

Table 1 Extra (conical) volume (V_e) of alkanethiolate-protected gold (C_n Au) nanoparticles (core diameter 2 nm). Note that the capping ligand chainlength (d) is estimated by Hyperchem[®]; and n denotes the number of carbon in the alkyl chain

	C4Au	C5Au	C6Au	C7Au	C8Au	C9Au	C10Au
d/nm	0.51	0.65	0.77	0.89	1.02	1.14	1.28
V_e/nm^3	0.065	0.101	0.159	0.220	0.298	0.384	0.500

smaller than a single chainlength as assumed.

More interestingly, when the particle monolayer was transferred onto an IDA electrode surface by the LB technique, conductivity measurements exhibited even better-defined single electron transfer characters.³⁵ Fig. 3 (panels A and B) shows the solid-state I – V profiles and differential pulse voltammograms (DPVs) of an LB monolayer of C6Au nanoparticles deposited onto an IDA electrode surface at $L = 0.72 \text{ nm}$. The measurements were carried out *in vacuo* and at varied temperatures. When the temperature is controlled at 300 and 320 K, there are at least five pairs of well-defined and evenly spaced current peaks within the potential range of -1.0 to $+1.0 \text{ V}$ (panels A and B). *These are, again, attributable to the single electron*

transfer across the nanoparticle monolayers. From the potential spacing (0.27 V), the corresponding C_{PP} can be evaluated at 0.59 aF . Note that this is slightly larger than that obtained in Fig. 2 as the interparticle separation is smaller (data in Fig. 2 were also acquired at ambient temperature).

These discrete charge transfer features diminished abruptly at lower temperatures (160 to 280 K), though the monolayer conductance remained at least an order of magnitude greater than that of the blank electrode (panel C). Such a drastic change of ensemble conductivity cannot be accounted for by the thermal activation mechanism alone. Note that the melting temperature of the C6Au nanoparticle solids, as estimated in differential scanning calorimetric (DSC) measurements,³ is somewhat lower.

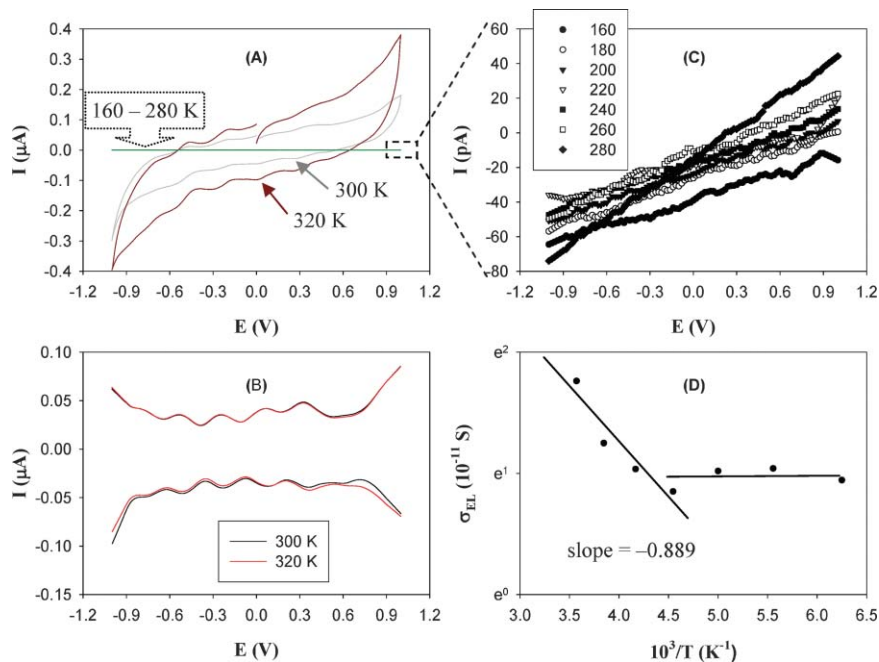


Fig. 3 (A) Current–potential (I – V) profiles of a C6Au nanoparticle monolayer deposited onto an IDA electrode surface by the LB technique at $L = 0.72 \text{ nm}$. The measurements were carried out *in vacuo* and at varied temperatures. Potential scan rate 20 mV s^{-1} . (B) Differential pulse voltammograms (DPV) at 300 and 320 K. Pulse amplitude 50 mV , pulse width 200 ms , dc ramp 20 mV s^{-1} . (C) Amplified I – V curves of those at 160 to 280 K as shown in (A). (D) Semilog plot of the electronic conductivity of the particle monolayers at varied temperatures (160 to 280 K). Symbols are experimental data collected from the I – V curves in (C). Lines are linear regressions. Reproduced with permission from Wiley (ref. 35).

While the detailed molecular origin is not clear at this point, it should be pointed out that a recent study¹⁴ shows that thermally induced particle core motions could lead to drastic enhancement of the ensemble conductance as a result of the modulation of interparticle separation. In fact, low frequency Raman scattering studies have shown that nanoparticle solids may exhibit vibrational collective coherence, with the frequency inversely proportional to the particle core diameter.³⁶ It is very plausible that a similar mechanism underlies the present observations.

Additionally, panel D depicts the temperature dependence of the particle film conductivity by assuming linear I - V behavior. Here Arrhenius behavior can be seen within the temperature range of 220 to 280 K, suggesting a *thermal activation* mechanism of the particle charge transfer, with an activation barrier of *ca.* 76.7 meV which is comparable to those with thick films of similar nanoparticles.^{37–39} At ambient temperatures (panel A, 300–320 K), the conductance also increases with increasing temperature. Thus, collectively, these observations imply that the monolayer conductance may be manipulated by temperature in at least two ways: (i) the energetic states of electrons that determine the charge transfer pathways, and (ii) the core motions that facilitate interparticle charge transfer.

By contrast, at even lower temperatures (160 to 200 K), the conductivity exhibits only a very weak temperature dependence, suggesting that the particle monolayer is highly insulating and the charge transfer is possibly arising from a *superexchange* mechanism. At low temperatures, the particle ensemble reaches the domain-localized regime, where the charge is delocalized over a finite but restricted number of states, such that the conductance occurs by virtue of effective coupling between two particles that are not necessarily adjacent but whose energies are almost degenerate. Similar variation of the charge transfer mechanism with temperature was also observed experimentally and computationally with larger AgSR nanoparticle arrays.⁴⁰ Furthermore, Ratner *et al.*⁴¹ recently reported that the electron-transfer mechanism within oligo-*p*-phenylene-based molecular wires exhibited a

transition from superexchange to hopping which was gated by the conformation of the chemical bridges, as manifested by the different temperature dependence of the resulting electron-transfer kinetics.

Thus, the above responses suggest that temperature is an important and delicate variable in the regulation of the charge-transfer dynamics of nanoparticle monolayers, by virtue of the combined effects of thermally induced structural transition of the particle films and thermal activation of interparticle electron transfer.⁴² Consequently, solid-state SETs only occur within a very narrow range of temperature where particle ensemble structure and interparticle electron transfer dynamics are optimized.

To examine the effects of the *electrode/particle interfacial contacts* on the ensemble conductance, we carried out further studies using the same electrode setup and depositing the particle monolayer at varied interparticle separations.³⁵ Fig. 4 depicts the I - V profiles at varied temperatures of a C6Au particle monolayer deposited at a shorter interparticle separation, $L = 0.62$ nm, where the I - V responses exhibit only linear (ohmic) characters within the entire temperature range of 160 to 320 K (and the conductance increases with increasing temperature). Since the electrode/particle contacts are essentially the same in these measurements as those in Fig. 3, the observed discrepancy of the I - V profiles strongly suggests that *the ensemble conductance is predominantly controlled by the particle assemblies rather than the interfacial contacts*. The featureless current response observed at this shorter interparticle spacing might be ascribed to

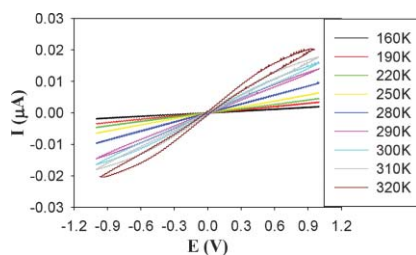


Fig. 4 I - V profiles at varied temperatures of a C6Au monolayer deposited at $L = 0.62$ nm. Other experimental conditions are the same as those in Fig. 3. Reproduced with permission from Wiley (ref. 35).

the enhanced electronic coupling between adjacent particles which leads to an increase of the particle-particle coupled capacitance (C_{PP}) and hence diminishment of the quantized charge transfer characters. The overall I - V profiles are in fact very similar to those with a dropcast thick film of the same C6Au particles.³⁵

It should be noted that the above experimental results represent the *first observations of single electron transfer across a particle solid thin film* (and the results are very reproducible).³⁵ The overall behavior is analogous to that of STM-based measurements of individual nanoparticles (both are in the two-electrode mode). The fact that discrete charge transfer can be observed even at moderate electrode potentials indicates that the electronic coupling between the particles should be relatively weak within the present experimental context and consequently the conductance of the particle monolayer has not reached the “metallic” domain. However, the electronic interactions should be strong enough to overcome the Coulombic barrier and consequently to initiate discrete charge transfer between neighboring particles. As the nanoparticle monolayers at the air/water interface can undergo a metal-insulator transition upon mechanical compression,^{4,22} these studies^{28,29,35} demonstrate that with deliberate control of the particle structures and interparticle interactions, lateral single electron transfer can also be achieved across these nanoparticle assemblies. In fact, the optimal interparticle separation was found to coincide with the particle arrangements where Anderson-like localized to delocalized transition occurred,⁴³ with a minimal energetic barrier for interparticle charge transfer.

Importantly, such unique SET characters are *defect-tolerant*, since there are inevitably structural defects (disordered domains) within the micron-sized particle ensembles that arise from the particle core size dispersity (<20%). Because of poor coupling and high resistance in these defect regions, the overall ensemble conductance will be dictated predominantly by the majority of particles that are in organized arrays (and hence low resistance). Thus, access to (structurally and compositionally)

monodisperse nanoparticles is imperative to maximize the ensemble conductance, which remains a continuing challenge.

So far the work has been mainly focused on gold nanoparticles, because of the ready availability of very small gold particles with narrow size dispersity. It is anticipated that similar discrete charge transfer behavior will be observed with other transition-metal nanoparticles within a similar size range (e.g., Ru,⁴⁴ Ag,⁴⁵ Pd,⁴⁶ etc) that have already been found to exhibit electrochemical quantized charging in electrolyte solutions. Yet for semiconductor nanoparticle solids, the main complication arises from the particle bandgap which results in minimum conductance within a very large potential range in I - V measurements.^{47,48} Whereas several approaches such as doping, electrical gating as well as optical excitation may be employed to manipulate the interparticle charge transfer, the parameter optimization for interparticle single electron transfer will be more challenging and complicated than for the metal nanoparticles mentioned above.

In addition, how the solid-state discrete charge transfer responds to external fields will provide a unique gating mechanism towards the development of single electron transistors and chemical sensors. For instance, when exposed to different solvent vapors, the conductance of a nanoparticle solid film may be modulated by the polarity of the solvents and consequently the solvation-induced ensemble swelling effects.^{14,49–51} Additionally, charge transport along a Pd nanowire has been found to be manipulated by pH when the wire surface is functionalized with ionizable moieties.⁵² The fundamental insights gained from these earlier studies can be exploited to chemically gate the single electron transfer of nanoparticle solids, which as demonstrated above is very sensitive to the ensemble structure and chemical environments. In these efforts, an understanding of the molecular mechanism is of fundamental significance in the further optimization of the ensemble structures and single electron transfer properties. It is anticipated that computational/theoretical tools and scanning probe microscopy/spectroscopy⁵³ will play an indispensable role in this effort.

In the long run, the approach demonstrated above may pave the way toward the development of nanoelectronic devices based on micron-scale ordered arrays of nanoparticles that can be easily fabricated.⁵⁴

Acknowledgements

The author is grateful for the contributions by his co-workers whose names are listed in the related references. This work was supported in part by the US National Science Foundation (CHE-0456130, and CHE-0718170), and the Petroleum Research Fund administered by the American Chemical Society (39729-AC5M).

References

- 1 M. Brust, M. Walker, D. Bethell, D. J. Schiffrin and R. Whyman, *J. Chem. Soc., Chem. Commun.*, 1994, 801.
- 2 R. L. Whetten, M. N. Shafiqullin, J. T. Khoury, T. G. Schaaff, I. Vezmar, M. M. Alvarez and A. Wilkinson, *Acc. Chem. Res.*, 1999, **32**, 397.
- 3 A. C. Templeton, M. P. Wuelfing and R. W. Murray, *Acc. Chem. Res.*, 2000, **33**, 27.
- 4 G. Markovich, C. P. Collier, S. E. Henrichs, F. Remacle, R. D. Levine and J. R. Heath, *Acc. Chem. Res.*, 1999, **32**, 415.
- 5 R. Shenhar and V. M. Rotello, *Acc. Chem. Res.*, 2003, **36**, 549.
- 6 M. C. Daniel and D. Astruc, *Chem. Rev.*, 2004, **104**, 293.
- 7 D. L. Feldheim and C. D. Keating, *Chem. Soc. Rev.*, 1998, **27**, 1.
- 8 U. Simon, *Adv. Mater.*, 1998, **10**, 1487.
- 9 D. I. Gittins, D. Bethell, D. J. Schiffrin and R. J. Nichols, *Nature*, 2000, **408**, 67.
- 10 R. P. Andres, T. Bein, M. Dorogi, S. Feng, J. I. Henderson, C. P. Kubiak, W. Mahoney, R. G. Osifchin and R. Reifenberger, *Science*, 1996, **272**, 1323.
- 11 S. W. Chen, *J. Electroanal. Chem.*, 2004, **574**, 153.
- 12 F. Remacle and R. D. Levine, *J. Am. Chem. Soc.*, 2000, **122**, 4084.
- 13 S. W. Chen, *Langmuir*, 2001, **17**, 6664.
- 14 J. P. Choi, M. M. Coble, M. R. Branham, J. M. DeSimone and R. W. Murray, *J. Phys. Chem. C*, 2007, **111**, 3778.
- 15 S. D. Evans, S. R. Johnson, Y. L. L. Cheng and T. H. Shen, *J. Mater. Chem.*, 2000, **10**, 183.
- 16 R. C. Doty, H. B. Yu, C. K. Shih and B. A. Korgel, *J. Phys. Chem. B*, 2001, **105**, 8291.
- 17 A. W. Snow and H. Wohltjen, *Chem. Mater.*, 1998, **10**, 947.
- 18 L. Clarke, M. N. Wybourne, L. O. Brown, J. E. Hutchison, M. Yan, S. X. Cai and J. F. W. Keana, *Semicond. Sci. Technol.*, 1998, **13**, A111.

- 19 G. N. R. Wang, L. Y. Wang, R. D. Qiang, J. G. Wang, J. Luo and C. J. Zhong, *J. Mater. Chem.*, 2007, **17**, 457.
- 20 A. Ulman, *An introduction to ultrathin organic films: from Langmuir-Blodgett to self-assembly*, Academic Press, New York, 1991.
- 21 G. Markovich, C. P. Collier and J. R. Heath, *Phys. Rev. Lett.*, 1998, **80**, 3807.
- 22 B. M. Quinn, I. Prieto, S. K. Haram and A. J. Bard, *J. Phys. Chem. B*, 2001, **105**, 7474.
- 23 A. J. Quinn, M. Biancardo, L. Floyd, M. Belloni, P. R. Ashton, J. A. Preece, C. A. Bignozzi and G. Redmond, *J. Mater. Chem.*, 2005, **15**, 4403.
- 24 M. Biancardo, A. J. Quinn, L. Floyd, P. M. Mendes, S. S. Briggs, J. A. Preece, C. A. Bignozzi and G. Redmond, *J. Phys. Chem. B*, 2005, **109**, 8718.
- 25 W. Y. Lee, M. J. Hostetler, R. W. Murray and M. Majda, *Isr. J. Chem.*, 1997, **37**, 213.
- 26 J. Kim and D. Lee, *J. Am. Chem. Soc.*, 2006, **128**, 4518.
- 27 S. W. Chen, R. W. Murray and S. W. Feldberg, *J. Phys. Chem. B*, 1998, **102**, 9898.
- 28 S. W. Chen, *Anal. Chim. Acta*, 2003, **496**, 29.
- 29 Y. Y. Yang, S. Pradhan and S. W. Chen, *J. Am. Chem. Soc.*, 2004, **126**, 76.
- 30 M. Fujihira and T. Araki, *Chem. Lett.*, 1986, 921.
- 31 D. R. Lide, *Handbook of Chemistry and Physics*, CRC, Boca Raton, FL, 1995.
- 32 C. P. Collier, T. Vossmeier and J. R. Heath, *Annu. Rev. Phys. Chem.*, 1998, **49**, 371.
- 33 J. R. Heath, C. M. Knobler and D. V. Leff, *J. Phys. Chem. B*, 1997, **101**, 189.
- 34 H. Sellers, A. Ulman, Y. Shnidman and J. E. Eilers, *J. Am. Chem. Soc.*, 1993, **115**, 9389.
- 35 S. Pradhan, J. Sun, F. J. Deng and S. W. Chen, *Adv. Mater.*, 2006, **18**, 3279.
- 36 M. P. Pileni, *Acc. Chem. Res.*, 2007, DOI: 10.1021/ar6000582.
- 37 R. H. Terrill, T. A. Postlethwaite, C. H. Chen, C. D. Poon, A. Terzis, A. D. Chen, J. E. Hutchison, M. R. Clark, G. Wignall, J. D. Londono, R. Superfine, M. Falvo, C. S. Johnson, E. T. Samulski and R. W. Murray, *J. Am. Chem. Soc.*, 1995, **117**, 12537.
- 38 W. P. Wuelfing, S. J. Green, J. J. Pietron, D. E. Cliffler and R. W. Murray, *J. Am. Chem. Soc.*, 2000, **122**, 11465.
- 39 M. Brust, D. Bethell, D. J. Schiffrin and C. J. Kiely, *Adv. Mater.*, 1995, **7**, 795.
- 40 F. Remacle, K. C. Beverly, J. R. Heath and R. D. Levine, *J. Phys. Chem. B*, 2003, **107**, 13892.
- 41 E. A. Weiss, M. J. Tauber, R. F. Kelley, M. J. Ahrens, M. A. Ratner and M. R. Wasielewski, *J. Am. Chem. Soc.*, 2005, **127**, 11842.
- 42 T. B. Tran, I. S. Beloborodov, X. M. Lin, T. P. Bigioni, V. M. Vinokur and H. M. Jaeger, *Phys. Rev. Lett.*, 2005, **95**, 076806.
- 43 F. Remacle, *J. Phys. Chem. A*, 2000, **104**, 4739.
- 44 W. Chen, J. R. Davies, D. Ghosh, M. C. Tong, J. P. Konopelski and S. W. Chen, *Chem. Mater.*, 2006, **18**, 5253.

- 45 M. C. Tong, W. Chen, J. Sun, D. Ghosh and S. W. Chen, *J. Phys. Chem. B*, 2006, **110**, 19238.
- 46 S. W. Chen, K. Huang and J. A. Stearns, *Chem. Mater.*, 2000, **12**, 540.
- 47 I. A. Greene, F. X. Wu, J. Z. Zhang and S. W. Chen, *J. Phys. Chem. B*, 2003, **107**, 5733.
- 48 S. Pradhan, S. W. Chen, S. Z. Wang, J. Zou, S. M. Kauzlarich and A. Y. Louie, *Langmuir*, 2006, **22**, 787.
- 49 F. J. Ibanez, U. Gowrishetty, M. M. Crain, K. M. Walsh and F. P. Zamborini, *Anal. Chem.*, 2006, **78**, 753.
- 50 L. Y. Wang, X. J. Shi, N. N. Kariuki, M. Schadt, G. R. Wang, Q. Rendeng, J. Choi, J. Luo, S. Lu and C. J. Zhong, *J. Am. Chem. Soc.*, 2007, **129**, 2161.
- 51 W. H. Steinecker, M. P. Rowe and E. T. Zellers, *Anal. Chem.*, 2007, **79**, 4977.
- 52 M. H. Yun, N. V. Myung, R. P. Vasquez, C. S. Lee, E. Menke and R. M. Penner, *Nano Lett.*, 2004, **4**, 419.
- 53 S. W. Chen, L.-P. Xu, S. Pradhan and W. Chen, *Solid State Commun.*, 2007, in press.
- 54 J. Z. Zhang, Z. L. Wang, J. Liu, S. W. Chen and G.-y. Liu, *Self-assembled nanostructures*, Kluwer Academic/Plenum Publishers, New York, 2003.

Find a SOLUTION

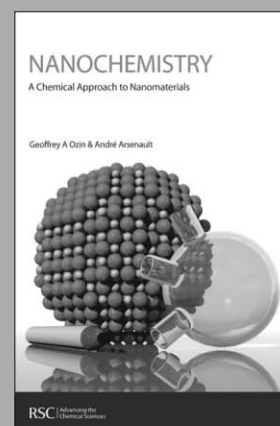
... with books from the RSC

Choose from exciting textbooks, research level books or reference books in a wide range of subject areas, including:

- Biological science
- Food and nutrition
- Materials and nanoscience
- Analytical and environmental sciences
- Organic, inorganic and physical chemistry

Look out for 3 new series coming soon ...

- RSC Nanoscience & Nanotechnology Series
- Issues in Toxicology
- RSC Biomolecular Sciences Series



RSC | Advancing the
Chemical Sciences

www.rsc.org/books